Biophysical Chemistry 140 (2009) 1–8

Contents lists available at ScienceDirect

Biophysical Chemistry

journal homepage: http://www.elsevier.com/locate/biophyschem

Electronic structures, DNA-binding and spectral properties of Co(III) complexes $[Co(bpy)_2(L)]^{3+}$ (L=pip, odhip, hnoip)

Ti-Fang Miao, Si-Yan Liao, Li Qian, Kang-Cheng Zheng *, Liang-Nian Ji

The Key Laboratory of Bioinorganic and Synthetic Chemistry of Ministry of Education, School of Chemistry and Chemical Engineering, Sun Yat-Sen University, Guangzhou 510275, China

ARTICLE INFO

Article history:
Received 11 September 2008
Received in revised form 24 October 2008
Accepted 5 November 2008
Available online 7 December 2008

Keywords:
Co(III) complex
Electronic structure
DNA-binding
Spectral property
DFT calculation

ABSTRACT

Studies on the electronic structures and trend in DNA-binding affinities of a series of Co(III) complexes have been carried out, using the density functional theory (DFT) at the B3LYP/LanL2DZ level. The optimized geometric structures of these Co(III) complexes in aqueous solution are more close to experimental data than those in vacuo. The electronic structures of these Co(III) complexes were analyzed on the basis of their geometric structures optimized in aqueous solution, and the trend in the DNA-binding constants (K_b) was reasonably explained. In addition, the electronic absorption spectra of these complexes were calculated and simulated in aqueous solution using the time dependent DFT (TDDFT) at the B3LYP/LanL2DZ level. The calculated absorption spectra of these Co(III) complexes in aqueous solution are in satisfying agreement with experimental results, and the properties of experimental absorption bands have been theoretically explained in detail. Meanwhile, in order to explore the solvent effect on the absorption spectra of these Co(III) complexes, their absorption spectra in vacuo were also calculated, and the results show that the calculated absorption spectra of Co(III) complexes are greatly influenced by the solvent effect.

1. Introduction

DNA plays a very important role in the life process, because it is the carrier of genetic information and its configuration exhibits polymorphism. DNA is a particularly good target for metal complexes as its base-pairs owns rich electrons. Therefore, transition metal complexes can bind to DNA in many modes such as electrostatic, groove and intercalative binding, etc. Among them, the intercalative mode is the most important mode in which transition metal complexes can intercalate between the pair-bases of double helix DNA, forming π–π overlapping interaction. It is this interaction that greatly affects and/or damages DNA conventional behavior and so that these transition metal complexes possess a very broad application background in the field of bio-inorganic chemistry [1–5]. For example, the well-known Ru(II) polypyridyl-type complexes can used widely in probes of DNA structure, DNA-dependent electron transfer, DNA-molecular "light switches", DNA-photocleavage reagents and anticancer drugs [1]. Co(III) polypyridyl-type complexes have many attractive behaviors similar to Ru(II) polypyridyl-type complexes, and thus also attract most interests. Recently, many Co(III) polypyridyl complexes have been synthesized and characterized, and their DNA-binding properties were also investigated by UV–vis absorption spectra, emission spectra, viscosity measurements, circular dichroism spectra and gel electrophoresis experiments, etc [6–18]. In particular, Co(III) complex $[Co(bpy)_2(pip)]^{3+}$ (pip=2-phenylimidazo[4,5-*f*] [1,10]-phenanthroline) and its derivatives, have been found to possess excellent DNA-binding affinity, DNA-photocleavage ability as well as many other valuable biochemical functions, and thus more and more studies on Co(III) polypyridyl complexes have been carrying out [19]. It is very interesting that modifying the polypyridine ligands can usually create some unique differences in the DNA-binding properties of the resulting complexes [20,21]. Therefore, recently in order to develop novel molecular Co(III) complexes, some substituents were introduced on the main ligand (or called intercalative ligand) of some parent complexes, e.g., the ligand pip of $[Co(bpy)_2(pip)]^{3+}$ [22–24]. The DNA-binding behaviors of these derivatives as well as their spectral properties hopefully applied in DNA-molecular "light switches" and DNA-photocleavage reagents, closely relate to their electronic structures. However, so far as we know, the theoretical reports based on the electronic structures of Co(III) complexes to explain the DNA-binding regularity (or trend) as well as spectral properties remain quite infrequent, though the theoretical studies on the Ru(II) polypyridyl complexes have been quite frequently reported [25–30]. Since Co(III) ion carries more charges than Ru(II) ion, the Co(III) polypyridyl-type complexes should possess some owned characteristics different from Ru(II) polypyridyl complexes. Therefore, the theoretical studies on the electric structures, the related DNA-binding and spectral properties of these Co(III) polypyridyl-type complexes are still very significant works for directing the functional molecular design of transition metal complexes as well as the action mechanism analysis.

On the other hand, in recent years, time dependent density functional theory (TDDFT) has become a useful tool for the

* Corresponding author. Tel.: +86 20 84110696; fax: +86 20 84112245.
E-mail address: ceszkc@mail.sysu.edu.cn (K.-C. Zheng).

0301-4622/$ – see front matter © 2008 Elsevier B.V. All rights reserved.
doi:10.1016/j.bpc.2008.11.007

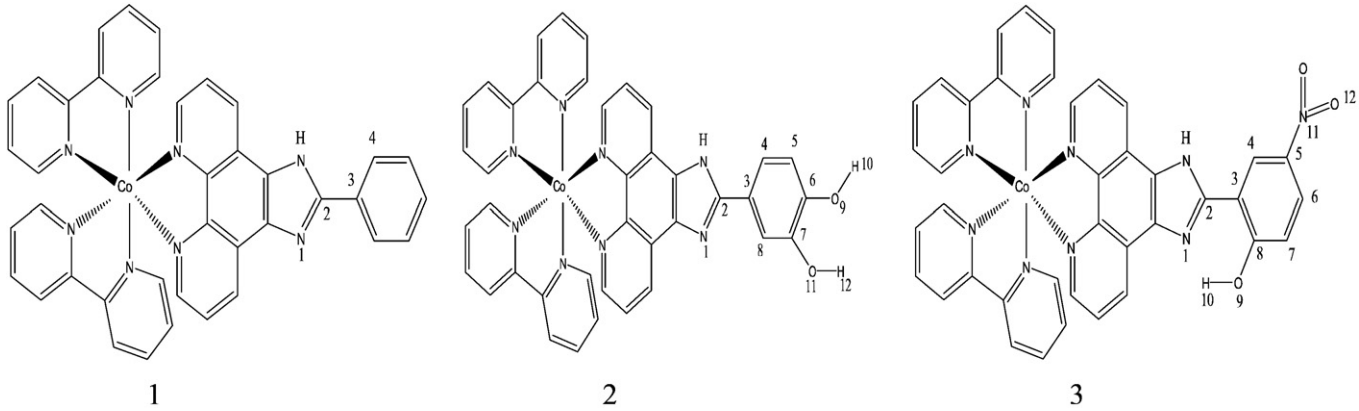

Fig. 1. Structural diagrams of the complexes **1–3** and atomic labels.

calculations of various molecule properties, such as electronic excitations, magnetic properties or polarizabilities in medium and larger molecule system, due to its good accuracy and reasonable computational cost [31–34]. The TDDFT method introduces errors by using approximate exchange-correlation (XC) functionals and fails in the excited states for long-range charge transition, but it can be solved by using approximate functionals corrected for long-range effects [35–38]. Recently, we have reported some TDDFT studies on spectral properties of Ru(II) polypyridyl complexes. Moreover, the computed results are in good agreement with the experimental ones, and thus provide considerable explanations and predictions for the experimental findings [25–28,39,40].

In this paper, the theoretical studies on the complex $[Co(bpy)_2(pip)]^{3+}$ [19] and its substitutive derivatives $[Co(bpy)_2(L)]^{3+}$ (L=odhip, hnoip) (odhip=3, 4-dihydroxyl-imidazo[4,5-*f*] [1,10]phenanthroline, hnoip=2-(2-hydroxy-5-nitrophenyl) imidazo [4,5-*f*] [1,10]phenanthroline) [22,23] applying the DFT method are carried out. The effects of some substituents on the intercalative ligand (pip) on the geometric and electronic structures of the resulting complexes are investigated. This paper is mainly focused on theoretically explaining the trend in DNA-binding affinities of this series of complexes. In addition, the absorption spectra of the complexes in aqueous solution are also computed, simulated, and discussed by the TDDFT method.

2. Computational methods

The studied complexes are shown in Fig. 1. Every one of the complexes $[Co(bpy)_2(L)]^{3+}$ (L=pip, odhip, hnoip) forms from Co(III) ion, one main ligand (or called as intercalative ligand) (L), and two co-ligands (bpy), and has no symmetry. Full geometry optimization of the complexes in ground state (S_0) was carried out in aqueous solution using the restricted DFT-B3LYP method and LanL2DZ basis set [41,42]. For the obtained structures, the frequency calculations adopting the same method were also performed in order to verify the optimized structure to be an energy minimum. On the basis of the DFT optimized ground geometry, the electronic absorption spectra in aqueous solution were calculated with the time-dependent theory (TDDFT) at the level of B3LYP/LanL2DZ. 180 singlet-excited-state energies of these complexes were calculated to reproduce electronic absorption spectra. The conductor polarizable continuum model (CPCM) [43,44] was applied to the solvent effect in aqueous solution. To explore the solvent effect on the electronic structures and related properties, the calculations of these complexes in vacuo were also carried out adopting the same method. All the calculations were performed by means of the Gaussian03 program-package (revision D.01) [45]. In addition, in order to clearly depict the detail of some frontier molecular orbitals of these complexes in ground state, their stereo-contour graphs were drawn with the Molden v4.2 [46] program based on the DFT computational results.

3. Results and discussion

3.1. Ligand effects on selected bond lengths and bond angles of the complexes

The calculated geometrical parameters of complexes **1–3** are selectively listed in Table 1. For comparison, the corresponding X-ray data of the analog $[Co(phen)_3](ClO_4)_3$ [47] are also given in Table 1.

Since the crystal structures of the three complexes have not been determined yet, the direct comparison between the computational results and the corresponding experimental data cannot be performed. However, according to the comparison between the calculated results and experimental data of the analog $[Co(phen)_3](ClO_4)_3$, we can find that the computed mean bond lengths ($Co–N_m$ and $Co–N_{co}$) are 1.981 Å in vacuo and 1.968 Å in aqueous solution by the DFT method. These calculated bond lengths are slightly longer than the corresponding

Table 1
Computed selective bond lengths (Å), bond angles (°) and dihedral angles (°) of the complexes in vacuo and in aqueous solution using the DFT at the B3LYP/LanL2DZ level

Comp.	$Co–N_m^a$	$Co–N_{co}^a$	$C–C(N)_m^b$	$C–C(N)_{co}^b$	θ_m^c	θ_{co}^c	Dihedral angle		
$[Co(phen)_3]^{3+}$	1.981	1.981	1.405	1.405	84.1	84.1			
$^*[Co(phen)_3]^{3+}$	1.968	1.968	1.403	1.403	84.7	84.7			
Expt [47]	1.943	1.943							
1 (L=pip)	1.977	1.972	1.405	1.399	84.2	83.0	179.91^{β}		
***1** (L=pip)	1.970	1.959	1.404	1.398	83.6	84.0	-179.22^{β}		
2 (L=odhip)	1.976	1.972	1.405	1.399	84.2	83.1	-179.33^{β}	180.00^{γ}	-179.98^{ε}
***2** (L=odhip)	1.969	1.960	1.404	1.398	84.4	83.6	-177.59^{β}	179.94^{γ}	179.80^{ε}
3 (L=hnoip)	1.980	1.971	1.407	1.399	84.0	83.1	-179.99^{β}	179.92^{φ}	179.96^{δ}
***3** (L=hnoip)	1.971	1.958	1.404	1.398	84.2	83.6	-179.92^{β}	179.74^{φ}	179.77^{δ}

[a] $Co–N_m$ is the average coordination bond length between the central atom and the main ligand (L), and $Co–N_{co}$ is that between the central atom and the co-ligand (bpy). [b] $C–C(N)_m$ is the mean bond length of skeleton of the main ligand, and $C–C(N)_{co}$ is that of the co-ligands (bpy). [c] θ_m is the coordination bond angle of the central atom and the two N atoms of the main ligand, and θ_{co} is that of the central atom and the two N atoms of the co-ligands (bpy), β is the dihedral angle $N_1–C_2–C_3–C_4$. γ, ε, φ and δ are the dihedral angles $C_7–C_6–O_9–H_{10}$, $C_8–C_7–O_{11}–H_{12}$, $C_4–C_5–N_{11}–O_{12}$ and $C_7–C_8–O_9–H_{10}$, respectively. *: The complexes with "*" and without "*" express the calculations in aqueous solution and in vacuo, respectively.

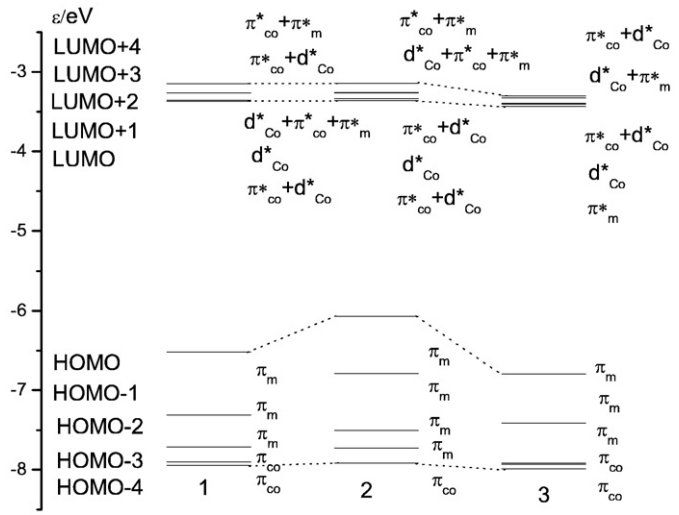

Fig. 2. Energies of some frontier molecular orbitals of complexes **1–3** in aqueous solution at the B3LYP/LanL2DZ level.

experimental value (1.943 Å). Comparing the calculated geometrical parameters of the $[Co(phen)_3]^{3+}$ in vacuo and in aqueous solution with corresponding X-ray data, we can clearly see that the calculated results in aqueous solution are quite better than those in vacuo. Therefore, it can be reasonably deduced that the solvent effect is very important for the calculations of this kind of Co(III) complex with high positive charges.

Table 1 gives the computational selected geometric parameters of the ground-state complexes **1–3** in vacuo and in aqueous solution. From computational geometric parameters in aqueous solution in Table 1, we can see the following: First, the coordination bond length (1.969–1.971 Å) of the main ligand for every one of complexes **1–3** is slightly longer than that (1.958–1.960 Å) of the co-ligands. Second, the mean bond length of the skeleton of the main ligand ($C–C(N)_m$) and that of the co-ligands ($C–C(N)_{co}$) for complexes **1–3** are almost unchanged, and the former is only slightly longer than the latter for every one of complexes **1–3**. Third, although all related dihedral angles (listed in Table 1) of these complexes are close to ±180.0°, there is a detectable difference among the dihedral angles (β) of complexes **1–3**, that is, the dihedral angles (β) of complexes **1–3** are −179.22 °, −177.59 ° and −179.92 °, respectively. Such a fact shows that the planarity of the main-ligand of the complex **2** is worse than those of complexes **1** and **3**, and thus the steric hindrance of its main-ligand intercalating between DNA-base-pairs must be bigger than those of complexes **1** and **3**.

In addition, from the optimized results of complexes **1–3**, we can also see that their dipole moments are 13.97, 17.83 and 30.92 Debye in vacuo and 22.07, 27.13 and 41.33 Debye in aqueous solution, respectively. Such a result shows that the values of dipole moments of complexes **1–3** in aqueous solution are markedly greater than those in vacuo, and proves further that the solvent has an important effect on the electronic and geometric structures of this kind of Co(III) complex with high positive charges.

3.2. Theoretical explanation of the trend in DNA-binding affinities of the complexes

The intrinsic binding constants K_b of the complexes **1–3** to calf thymus (CT) DNA, which quantitatively express their DNA-binding affinities, have been experimentally measured. The results show that the trend in DNA-binding constants (K_b) of the three complexes is K_b (**2**, 7.9×10^4 M^{-1})<K_b(**1**, 1.9×10^5 M^{-1})<K_b(**3**, 2.06×10^5 M^{-1}) [19,23,48]. Such a trend can be reasonably explained by the DFT calculations.

As is well-known, there are π–π stacking interactions between the complex and DNA-base-pairs while the complex binds to DNA in an intercalation (or part intercalation) mode [1,49]. Moreover, many theoretical studies have shown the following idea: (1) The DNA base-pairs are electron donors and an intercalated complex is an electron acceptor. (2) The energies of HOMO and HOMO −x (x: small integer) of DNA-base-pairs are rather high, and their components are predominately distributed on DNA-base-pairs [50,51]. (3) The energies of LUMO and LUMO+x of the intercalated complex are all negative and rather low, and even quite lower than those of HOMO−x of DNA-base-pairs, and their components are generally distributed on the main ligand of the complex. Since the DNA base-pairs as electron-donor are unchanged in our study, from the above analysis, we can see that the key factor affecting DNA-binding affinities of the complexes should be the energy and population of the lowest unoccupied molecular orbital (LUMO, even and LUMO+x) of the intercalated molecules [52–54]. In addition, the planarity of the complex molecule should also be considered. Hereby, the above-mentioned trend in DNA-binding, i.e, K_b(**2**)<K_b(**1**)<K_b(**3**), can be explained as follows: First, the energies of the LUMO+x (x=0–4) of these complexes are all rather low negative values (see Fig. 2), suggesting that these complexes are very excellent electron acceptors in their DNA-binding. Second, the LUMO energies (ε_{LUMO}) follow the sequence of ε_{LUMO} (**2**, −3.363 eV)≈ε_{LUMO} (**1**, −3.369 eV)>ε_{LUMO} (**3**, −3.435 eV). Moreover, from Fig. 3, we can see that there are always some LUMO+x on which the π-components of intercalative ligands are predominantly populated. A lower LUMO energy of complex is advantageous to accepting the electrons from DNA base pairs in an intercalative mode, because electrons or "electron-cloud" can transfer from HOMO of DNA-base-pairs to LUMO of the complex via inter-overlapping orbitals. So we can preliminarily predict that the trend in DNA-binding constants (K_b) of these complexes is K_b(**3**)>K_b(**1**)≈K_b(**2**) via the analysis in LUMO energies. Third, from the geometric parameters of these complexes (see Table 1), although the planarity and conjugated area of the main-ligand skeletons of complexes **1–3** are not substantially different, the steric hindrance of the main ligand of complex **2** in the intercalative mode should be bigger than those of complexes **1** and **3** because the important dihedral angle β ($N_1–C_2–C_3–C_4$) of main-ligand of complex **2** is obviously greater than those of complexes **1** and **3** in aqueous solution (see Table 1). So we can predict that the DNA-binding constant of complex **2** [K_b(**2**)] should be the smallest. In a word, synthetically considering LUMO energy and steric hindrance, the trend in DNA-binding affinities, i.e., K_b(**3**)>K_b(**1**)>K_b(**2**), can be reasonably explained.

In summary, from the above analysis, it can be seen that the substitution of an electron-withdrawing and π-planar-keeping group for H on the intercalative ligand is much more advantageous to reducing the energies of LUMO+x and thus to improving the DNA-binding affinity of the substituted complex.

3.3. Theoretical explanation on the spectral properties

The experimental absorption spectra of Co(III) complexes in aqueous solution shows the presence of the band of comparable intensity, lying in the range of 200–400 nm, and such bands are mainly assigned to a ligand-to-ligand π–π* transition of the coordinated groups [6,19,22–24]. The calculated excitation energies (ΔE/eV) within the range 200–400 nm, oscillator strengths (f≥0.20) and main orbital transition contributions (≥12%) of the three complexes in aqueous solution with the TDDFT at the level of B3LYP/LanL2DZ, as well as the experimental values are given in Table 2. In addition, the simulated absorption spectra in aqueous solution and in vacuo are given in Fig. 4(a,b), and the corresponding experimental absorption spectra are also given in Fig. 4(c).

From Table 2, we can find for complex **1** in aqueous solution, five strong transitions with f>0.2 lie in the range of 200–400 nm. Among

them, the three bands at 309.1 nm, 288.7 nm and 275.9 nm mainly involve HOMO→LUMO+9; HOMO−5→LUMO+4; HOMO−4→LUMO+4; HOMO−2→LUMO+5; and they can mainly be characterized by $\pi_m \rightarrow \pi^*_{co} + \pi^*_m$ and $\pi_{co} \rightarrow \pi^*_m + \pi^*_{co}$. The experimental broad band at 293 nm can be assigned to a superposition of these three bands with a ligand-to-ligand transition ($\pi \rightarrow \pi^*$) feature. The other bands at 200.0 nm and 227.0 nm mainly involve HOMO−8→LUMO+6 and HOMO−13→LUMO+1, and they can be respectively characterized by $\pi_{co} \rightarrow \pi^*_{co}$ and $\pi_{co} \rightarrow d^*_{Co}$. The experimental band observed at 223 nm can be assigned to a superposition of the two bands with ligand-to-ligand transition ($\pi \rightarrow \pi^*$) and ligand-to-metal charge transfer (LMCT) characters.

For the spectra of complex **2** in aqueous solution, first, the experimental band at 305 nm can be assigned to a superposition of the bands at 333.5 nm (f=0.624), 284.1 nm (f=0.338) and 277.1 nm (f=0.464). These bands mainly involve the orbital transitions of HOMO−4→LUMO+10, HOMO−2→LUMO+5 and HOMO−3→LUMO+5, respectively. From Fig. 3, we can see that the above three orbital transitions possess a $\pi \rightarrow \pi^*$ feature of ligand-to-ligand (LL) transition. Second, the experimental band observed at 221 nm can also be assigned to a superposition of the strong bands at 226.6 nm (f=0.212) and 220.2 nm (f=0.316), which mainly involve the orbital transitions of $\pi \rightarrow \pi^*$ with a ligand-to-ligand (LL) feature.

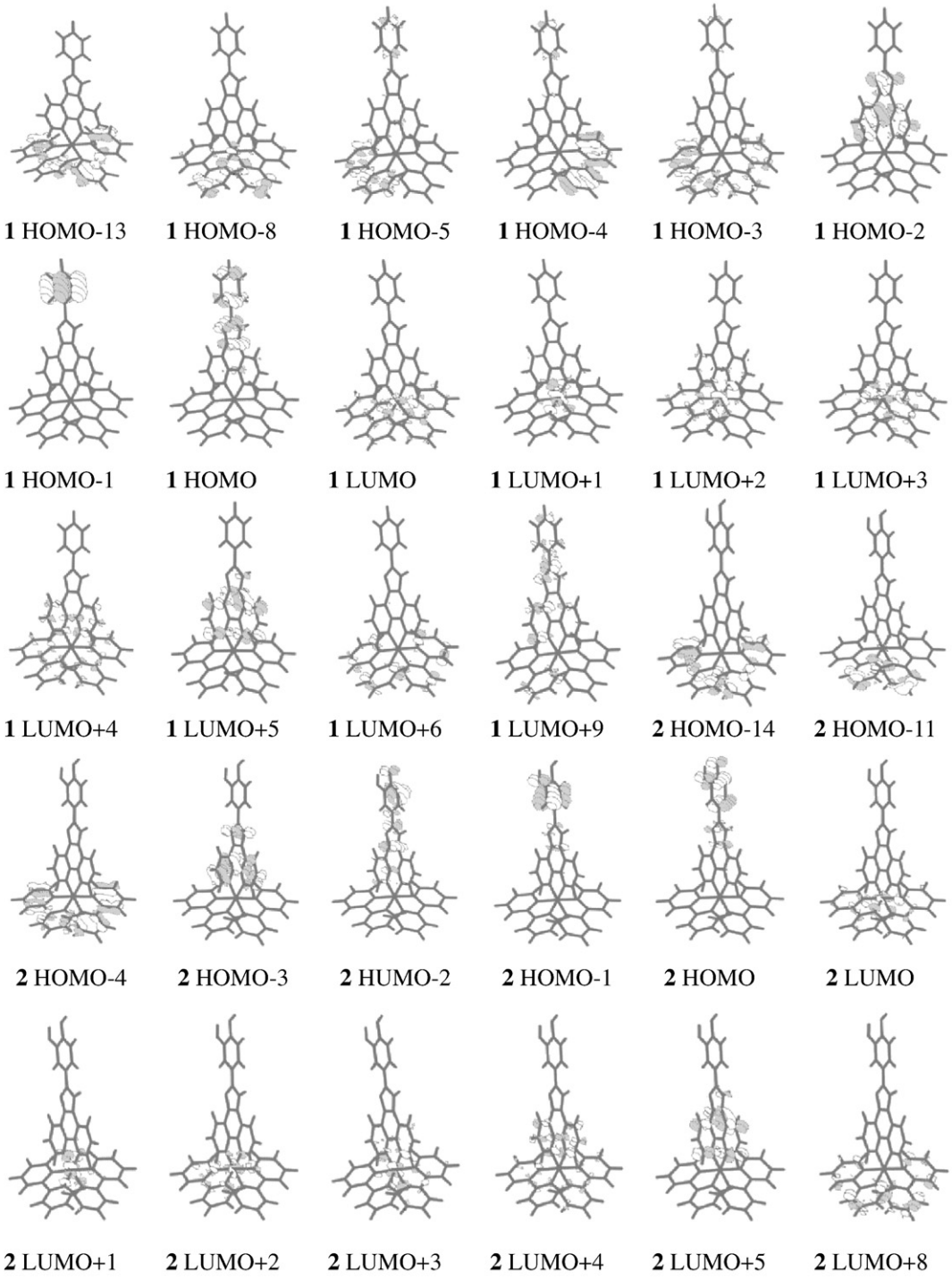

Fig. 3. Steric contour plots of some frontier molecular orbitals of complexes **1–3** in aqueous solution using the DFT method at the B3LYP/LanL2DZ level.

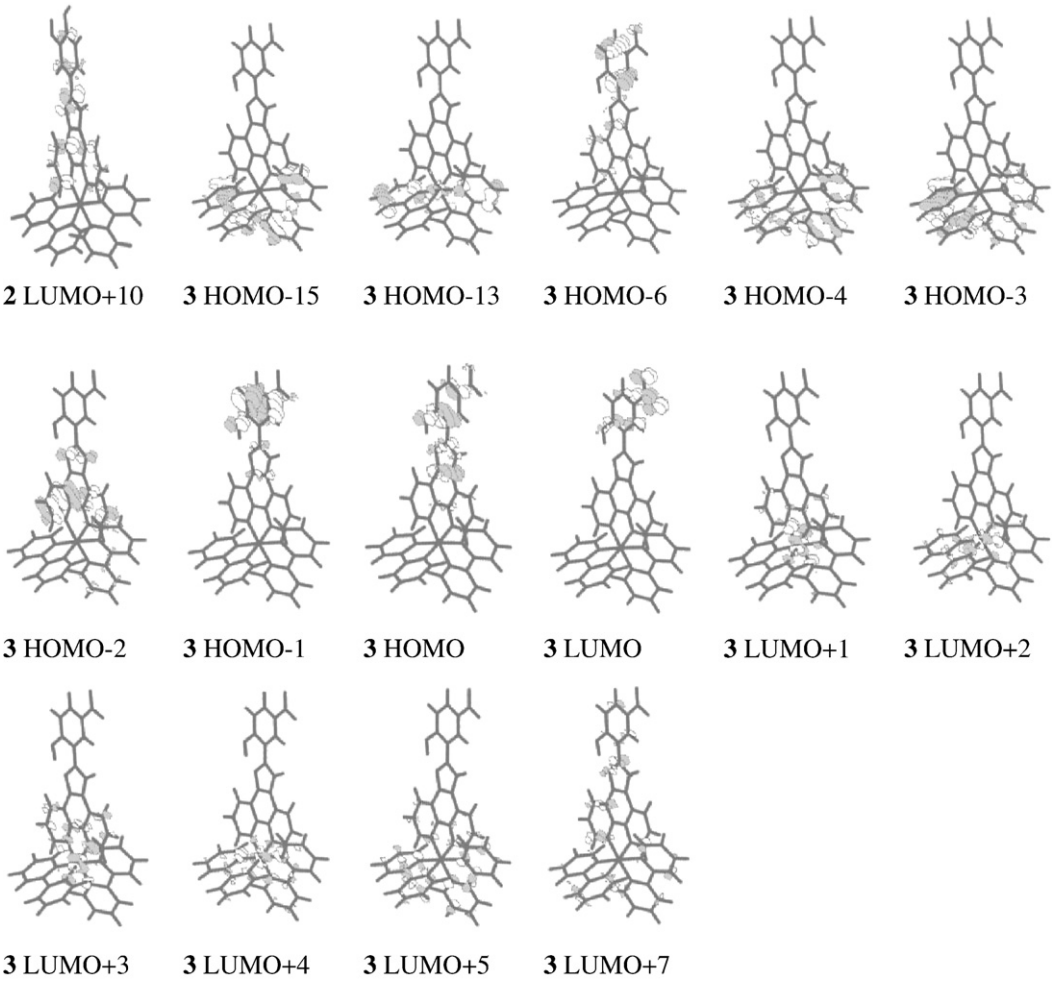

Fig. 3 (*continued*).

For the spectra of complex **3** in aqueous solution, the experimental band observed at 308 nm can be assigned to a superposition of five strong bands at 348.1 nm (f=0.326), 320.6 nm (f=0.504), 288.9 nm (f=0.296), 271.5 nm (f=0.214) and 263.9 nm (f=0.220), and all orbital transitions possess a $\pi \rightarrow \pi^*$ feature of ligand-to-ligand (LL) transition and minor $\pi \rightarrow d^*$ feature of ligand-to-metal charge transfer (LMCT) transition. Furthermore, the experimental band observed at 228 nm can also be assigned to the strong band at 226.4 nm (f=0.232). This

Table 2
Calculated excitation energies (ΔE/eV), oscillator strengths ($f \geq 0.20$), and main orbital transition contributions (≥12%) of complexes **1**–**3** in aqueous solution as well as the experimental values [19,22,23]

No	Major contribution	ΔE/eV	f	λ/nm (calc.)	λ/nm (expt.)	Character
1	H→L+9	4.01	0.533	309.1	293	$\pi_m \rightarrow \pi^*_{co} + \pi^*_m$
	H−5→L+4	4.29	0.234	288.7		$\pi_{co} \rightarrow \pi^*_m + \pi^*_{co}$
	H−4→L+4					$\pi_{co} \rightarrow \pi^*_m + \pi^*_{co}$ $\pi_m \rightarrow \pi^*_{co}$ or $\pi_m \rightarrow \pi^*_m$
	H−2→L+5	4.49	0.617	275.9		$\pi_m \rightarrow \pi^*_m$
	H−13→L+1	5.46	0.257	227.0	223	$\pi_{co} \rightarrow d^*_{Co}$
	H−8→L+6	6.20	0.259	200.0		$\pi_{co} \rightarrow \pi^*_{co}$ $d_{Co} \rightarrow \pi^*_{co}$
2	H−4→L+10	3.72	0.624	333.5	305	$\pi_{co} \rightarrow \pi^*_m$
	H−2→L+5	4.36	0.338	284.1		$\pi_m \rightarrow \pi^*_m$
	H−3→L+5	4.47	0.464	277.1		$\pi_m \rightarrow \pi^*_m$
	H−4→L+8	5.47	0.212	226.6		$\pi_{co} \rightarrow \pi^*_{co}$
	H−14→L+2	5.63	0.316	220.2	221	$\pi_{co} \rightarrow d^*_{Co}$
	H−11→L+4					$\pi_{co} \rightarrow \pi^*_m + \pi^*_{co}$
3	H−1→L	3.56	0.326	348.1		$\pi_m \rightarrow \pi^*_m$
	H→L+7	3.87	0.504	320.6	308	$\pi_m \rightarrow \pi^*_m + \pi^*_{co}$
	H−4→L+5	4.29	0.296	288.9		$\pi_{co} \rightarrow \pi^*_{co}$
	H−1→L+7	4.57	0.214	271.5		$\pi_m \rightarrow \pi^*_{co} + \pi^*_m$
	H−6→L+1					$\pi_m \rightarrow d^*_{Co}$
	H−6→L+3	4.70	0.220	263.9		$\pi_m \rightarrow \pi^*_m + d^*_{Co}$
	H−15→L+3	5.47	0.232	226.4	228	$\pi_{co} \rightarrow \pi^*_m + d^*_{Co}$
	H−13→L+5					$\pi_{co} \rightarrow \pi^*_{co} + d_{Co} \rightarrow \pi^*_{co}$

band mainly involves the orbital transitions of HOMO−15→LUMO+3 and HOMO−13→LUMO+5, and they can be characterized by $\pi_{co}\rightarrow\pi^*_m+d^*_{Co}$ and $\pi_{co}\rightarrow\pi^*_{co}$ containing $d_{Co}\rightarrow\pi^*_{co}$.

The simulated absorption spectra of complexes **1–3** in vacuo are also given in Fig. 4(b). Comparing Fig. 4(a, b) with Fig. 4(c), we can clearly see that the simulated absorption spectra in aqueous solution are in satisfying agreement with the experimental results and those in vacuo quite deviate from the experimental results. Such a fact shows that the Co(III) complex is influenced greatly by the solvent effect and the solvent effect must be taken into careful

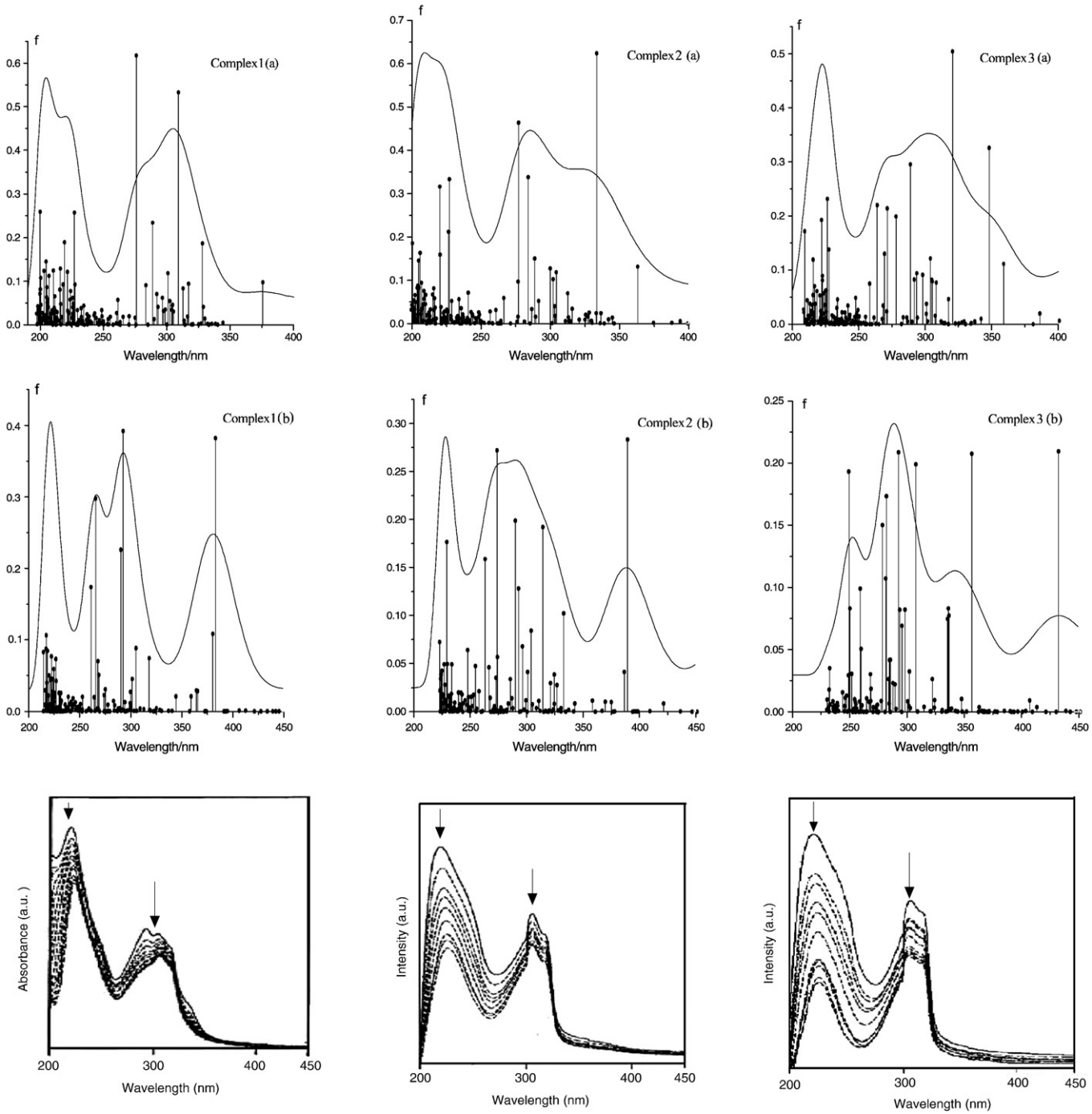

Absorption spectra of complex 1 (c) in the absence (–) and presence (---) of DNA with subtraction of the DNA absorbance.[19]

Absorption spectra of complex 2 (c) in the absence (–) and presence (---) of DNA with subtraction of the DNA absorbance.[22]

Absorption spectra of complex 3 (c) in the absence (–) and presence (---) of DNA with subtraction of the DNA absorbance.[23]

Fig. 4. The calculated absorption spectra of complexes **1–3** in aqueous solution (**a**) and vacuo (**b**) and corresponding experimental ones (**c** or the bottom).

account for the calculations of absorption spectra of the Co(III) complexes.

In summary, the absorption spectra of the three complexes can be simulated and discussed in detail by the TDDFT computations. The stronger bands, in particular at ~300 nm, of the three complexes are mainly attributed to the transitions of $\pi_m \rightarrow \pi^*_{co} + \pi^*_m$ or $\pi_{co} \rightarrow \pi^*_m + \pi^*_{co}$, which can be used to explain the intense absorption spectra involving ligand-to-ligand (LL) $\pi \rightarrow \pi^*$ transitions of cobalt complexes in experiments. We can also see that the errors of the calculated energies of spectral bands of these complexes in aqueous solution from experiment data lie within 20–40 nm. Such errors may originate from the following reasons: Besides the theoretical level of the TDDFT, the present solvent effect model may be related for applied to Co(III) complexes with higher charges in highly polar solvent. We hope to further investigate these effects in future.

4. Conclusions

The DFT studies of a series of complexes $[Co(bpy)_2(L)]^{3+}$ (L = pip, odhip, hnoip) **1**–**3** show that the substituents on the intercalative ligands have important effects on the electronic structures, trend in the DNA-binding affinities and spectral properties of these complexes. The studied results show the following: (1) The optimized geometric structures in aqueous solution are more close to experimental data than those optimized in vacuo. (2) The trend in DNA-binding affinities (K_b) of the complexes, that is, $K_b(\mathbf{2}) < K_b(\mathbf{1}) < K_b(\mathbf{3})$, can be reasonably explained by the DFT calculations. (3) The absorption-spectral bands in vacuo and in aqueous solution have theoretically been calculated, simulated and assigned. The results show that the Co(III) complexes are greatly influenced by the solvent effect and the calculated absorption spectra of the Co(III) complexes in aqueous solution are in satisfying agreement with the experimental results.

Acknowledgment

We are heartily grateful to the National Natural Science Foundation of China for the financial support (No. 20673148).

References

[1] L.N. Ji, X.H. Zou, J.G. Liu, Shape- and enantioselective interaction of Ru(II)/Co(III) polypyridyl complexes with DNA, Coord. Chem. Rev. 216–217 (2001) 513–536.
[2] P. Zhao, L.C. Xu, J.W. Huang, K.C. Zheng, J. Liu, H.C. Yu, L.N. Ji, DNA binding and photocleavage properties of a novel cationic porphyrin-anthraquinone hybrid, Biophys. Chem. 134 (2008) 72–83.
[3] S. Dhar, M. Nethaji, A.R. Charkravarty, Steric protection of a photosensitizer in a *N*,*N*-Bis[2-(2-pyridyl)ethyl]-2-phenylethylamine-copper(II) bowl that enhances red light-induced DNA cleavage activity, Inorg. Chem. 44 (2005) 8876–8883.
[4] P. Zhao, L.C. Xu, J.W. Huang, K.C. Zheng, B. Fu, H.C. Yu, L.N. Ji, Tricationic pyridium porphyrins appending different peripheral substituents: experimental and DFT studies on their interactions with DNA, Biophys. Chem. 135 (2008) 102–109.
[5] R.S. Kumar, S. Arunachalam, Synthesis, micellar properties, DNA binding and antimicrobial studies of some surfactant–cobalt(III) complexes, Biophys. Chem. 136 (2008) 136–144.
[6] C.F. Zhou, X.S. Du, H. Li, Studies of interactions among cobalt(III) polypyridyl complexes, 6-mercaptopurine and DNA, Bioelectrochemistry 70 (2007) 446–451.
[7] T.B. Lu, G. Yang, L.N. Ji, Complexation of cobalt(II) perchlorate with crown ethers. Synthesis, properties and structure of complexes of cobalt(II) perchlorate with 16-crown-5 and its lariat derivatives, Transit. Met. Chem. 24 (1999) 375–379.
[8] S.Y. Niu, S.S. Zhang, L. Wang, X.M. Li, Hybridization biosensor using di(1,10-phenanthroline) (imidazo[*f*]1,10-phenanthroline)cobalt(II) as electrochemical indicator for detection of human immunodeficiency virus DNA, J. Electroanal. Chem. 597 (2006) 111–118.
[9] C.V. Sastri, D. Eswaramoorthy1, L. Giribabu, B.G. Maiya, DNA interactions of new mixed-ligand complexes of cobalt(III) and nickel(II) that incorporate modified phenanthroline ligands, J. Inorg. Biochem. 94 (2003) 138–145.
[10] P.T. Selvi, M. Palaniandavar, Spectral, viscometric and electrochemical studies on mixed ligand cobalt(III) complexes of certain diimine ligands bound to calf thymus DNA, Inorg. Chim. Acta. 337 (2002) 420–428.
[11] R. Indumathy, S. Radhika, M. Kanthimathi, T. Weyhermuller, B.U. Nair, Cobalt complexes of terpyridine ligand: crystal structure and photocleavage of DNA, J. Inorg. Biochem. 101 (2007) 434–443.
[12] S. Ghosh, A.C. Barve, A.A. Kumbhar, A.S. Kumbhar, V.G. Puranik, P.A. Datar, U.B. Sonawane, R.R. Joshi, Synthesis, characterization, X-ray structure and DNA photocleavage by *cis*-dichloro bis(diimine) Co(III) complexes, J. Inorg. Biochem. 100 (2006) 331–343.
[13] H. Li, Z.H. Xu, L.N. Ji, W.S. Li, Interactions of polypyridyl cobalt complexes with DNA studied by rotating electrode methods, J. Appl. Electrochem. 35 (2005) 235–241.
[14] J.P. Zheng, Z. Li, A.G. Wu, H.L. Zhou, H.Y. Bai, Y.H. Song, The structural transition of DNA–Tris(1,10-phenanthroline) cobalt(III) complexes in ethanol–water solution, Biochem. Biophys. Res. Commun. 299 (2002) 910–915.
[15] L. J in, P. Yang, Synthesis and DNA binding studies of cobalt(III) mixed-polypyridyl complex, J. Inorg. Biochem. 68 (1997) 79–83.
[16] S.K. Gupta, P.B. Hitchcock, Y.S. Kushwah, G.S. Argal, Synthesis, structure and DNA binding studies of a mononuclear cobalt(III) complex with a NNO donor Schiff base derived from 4-methyl-2,6-dibenzoylphenol and ethane-1,2-diamine, Inorg. Chim. Acta. 360 (2007) 2145–2152.
[17] X.L. Wang, H. Chao, H. Li, X.L. Hong, Y.J. Liu, L.F. Tan, L.N. Ji, DNA interactions of cobalt(III) mixed-polypyridyl complexes containing asymmetric ligands, J. Inorg. Biochem. 98 (2004) 1143–1150.
[18] V.G. Vaidyanathan, B.U. Nair, Photooxidation of DNA by a cobalt(II) tridentate complex, J. Inorg. Biochem. 94 (2003) 121–126.
[19] Q.L. Zhang, H. Xu, H. Li, J. Liu, J.Z. Liu, L.N. Ji, Synthesis, DNA-binding and photocleavage studies of cobalt(III) mixed-ligand complexes, Transit. Met. Chem. 27 (2002) 149–154.
[20] B. Peng, H. Chao, B. Sun, H. Li, F. Gao, L.N. Ji, Synthesis, DNA-binding and photocleavage studies of cobalt(III) mixed-polypyridyl complexes: $[Co(phen)_2(dpta)]^{3+}$ and $[Co(phen)_2(amtp)]^{3+}$, J. Inorg. Biochem. 101 (2007) 404–411.
[21] Q.L. Zhang, J.G. Liu, H. Chao, G.Q. Xue, L.N. Ji, DNA-binding and photocleavage studies of cobalt(III) polypyridyl complexes: $[Co(phen)_2IP]^{3+}$ and $[Co(phen)_2PIP]^{3+}$, J. Inorg. Biochem. 83 (2001) 49–55.
[22] Q.L. Zhang, J.H. Liu, X.Z. Ren, H. Xu, Y. Huang, J.Z. Liu, L.N. Ji, A functionalized cobalt (III) mixed-polypyridyl complex as a newly designed DNA molecular lights witch, J. Inorg. Biochem. 95 (2003) 194–198.
[23] Q.L. Zhang, J.G. Liu, H. Xu, H. Li, J.Z. Liu, H. Zhou, L.H. Qu, L.N. Ji, Synthesis, characterization and DNA-binding studies of cobalt(III) polypyridyl complexes, Polyhedron 20 (2001) 3049–3055.
[24] Q.L. Zhang, J.G. Liu, J.Z. Liu, H. Li, Y. Yang, H. Xu, H. Chao, L.N. Ji, Effect of intramolecular hydrogen-bond on the DNA-binding and photocleavage properties of polypyridyl cobalt(III) complexes, Inorg. Chim. Acta. 339 (2002) 34–40.
[25] X.W. Liu, J. Li, H. Deng, K.C. Zheng, Z.W. Mao, L.N. Ji, Experimental and DFT studies on the DNA-binding trend and spectral properties of complexes $[Ru(bpy)_2L]^{2+}$ (L=dmdpq, dpq, and dcdpq), Inorg. Chim. Acta. 358 (2005) 3311–3319.
[26] J. Li, L.C. Xu, J.C. Chen, K.C. Zheng, L.N. Ji, Density functional theory/time-dependent DFT studies on the structures, trend in DNA-binding affinities, and spectral properties of complexes $[Ru(bpy)_2(p\text{-}R\text{-}pip)]^{2+}$(R= –OH, $-CH_3$, –H, $-NO_2$), J. Phys. Chem. A. 110 (2006) 8174.
[27] Z.Z. Xie, W.H. Fang, Electrophosphorescent divalent osmium and ruthenium complexes: a density functional theory investigation of their electronic and spectroscopic properties, J. Mol. Struct. (THEOCHEM) 717 (2005) 179–187.
[28] L.C. Xu, J. Li, Y. Shen, K.C. Zheng, L.N. Ji, Theoretical studies on the excited states, DNA photocleavage, and spectral properties of complex $[Ru(phen)_2(6\text{–}OH\text{–}dppz)]^{2+}$, J. Phys. Chem. A. 111 (2007) 273–280.
[29] J.C. Chen, L.M. Chen, S.Y. Liao, K.C. Zheng, L.N. Ji, A theoretical study on the hydrolysis process of the antimetastatic ruthenium(III) complex NAMI-A, J. Phys. Chem. B. 111 (2007) 7862–7869.
[30] L.C. Xu, S. Shi, J. Li, S.Y. Liao, K.C. Zheng, L.N. Ji, A combined computational and experimental study on DNA-photocleavage of Ru(II) polypyridyl complexes $[Ru(bpy)_2(L)]^{2+}$ (L=pip, o-mopip and p-mopip), Dalton trans (2008) 291–301.
[31] A. Dreuw, B.D. Dunietz, M. Head-Gordon, Characterization of the relevant excited states in the photodissociation of CO-ligated hemoglobin and myoglobin, J. Am. Chem. Soc. 124 (2002) 12070–12071.
[32] A. Tsolakidis, E. Kaxiras, A TDDFT study of the optical response of DNA bases, base pairs, and their tautomers in the gas phase, J. Phys. Chem. A. 109 (2005) 2373–2380.
[33] F. Mendizabal, B. Aguilera, C. Olea-Azar, Theoretical study on electronic spectra and aurophilic attraction in $[Au_3(MeN{=}COMe)_3]_4(n=1\text{–}4)$ complexes, Chem. Phys. Lett. 447 (2007) 345–351.
[34] T.F. Miao, S. Li, J.H. Cai, Theoretical study on magnetic and spectral properties of binuclear Copper(II) complexes, J. Mol. Struct. (THEOCHEM) 855 (2008) 45–51.
[35] A. Dreuw, M. Head-Gordon, Failure of time-dependent density functional theory for long-range charge-transfer excited states: the zincbacteriochlorin-bacteriochlorin and bacteriochlorophyll-spheroidene complexes, J. Am. Chem. Soc. 126 (2004) 4007–4016.
[36] A. Dreuw, M. Head-Gordon, Single-reference ab initio methods for the calculation of excited states of large molecules, Chem. Rev. 105 (2005) 4009–4037.
[37] M.J.G. Peach, P. Benfield, T. Helgaker, D.J. Tozer, Excitation energies in density functional theory: an evaluation and a diagnostic test, J. Chem. Phys 128 (2008) 044118-1–044118-8.
[38] D. Jacquemin, E.A. Perpète, G.E. Scuseria, I. Ciofini, C. Adamo, TD-DFT performance for the visible absorption spectra of organic dyes: conventional versus long-range hybrids, J. Chem. Theory Comput. 4 (2008) 123–135.
[39] J. Li, J.C. Chen, L.C. Xu, K.C. Zheng, L.N. Ji, A DFT/TDDFT study on the structures, trend in DNA-binding and spectral properties of molecular "light switch" complexes $[Ru(phen)_2(L)]^{2+}$ (L=dppz,taptp,phehat), J. Organomet. Chem. 692 (2007) 831–838.
[40] L.C. Xu, J. Li, S. Shi, K.C. Zheng, L.N. Ji, DFT/TDDFT studies on electronic absorption and emission spectra of $[Ru(bpy)_2(L)]^{2+}$ (L=pip, *o*-mopip and *p*-mopip) in aqueous solution, J. Mol. Struct. (THEOCHEM) 855 (2008) 77–81.
[41] P.J. Hay, W.R. Wadt, *Ab initio* effective core potentials for molecular calculations. Potentials for the transition metal atoms Sc to Hg, J. Chem. Phys. 82 (1985) 270–283.

[42] W.R. Wadt, P.J. Hay, *Ab initio* effective core potentials for molecular calculations. Potentials for main group elements Na to Bi, J. Chem. Phys. 82 (1985) 284–298.
[43] V. Barone, M. Cossi, Quantum calculation of molecular energies and energy gradients in solution by a conductor solvent model, J. Phys. Chem. A 102 (1998) 1995–2001.
[44] M. Cossi, N. Rega, G. Scalmani, V. Barone, Energies, structures, and electronic properties of molecules in solution with the C-PCM solvation model, J. Comp. Chem. 24 (2003) 669–681.
[45] M.J. Frisch, G.W. Trucks, H.B. Schlegel, G.E. Scuseria, M.A. Robb, J.R. Cheeseman, J.A. Montgomery Jr., T. Vreven, K.N. Kudin, J.C. Burant, J.M. Millam, S.S. Iyengar, J. Tomasi, V. Barone, B. Mennucci, M. Cossi, G. Scalmani, N. Rega, G.A. Petersson, H. Nakatsuji, M. Hada, M. Ehara, K. Toyota, R. Fukuda, J. Hasegawa, M. Ishida, T. Nakajima, Y. Honda, O. Kitao, H. Nakai, M. Klene, X. Li, J.E. Knox, H.P. Hratchian, J.B. Cross, V. Bakken, C. Adamo, J. Jaramillo, R. Gomperts, R.E. Stratmann, O. Yazyev, A.J. Austin, R. Cammi, C. Pomelli, J.W. Ochterski, P.Y. Ayala, K. Morokuma, G.A. Voth, P. Salvador, J.J. Dannenberg, V.G. Zakrzewski, S. Dapprich, A.D. Daniels, M.C. Strain, O. Farkas, D.K. Malick, A.D. Rabuck, K. Raghavachari, J.B. Foresman, J.V. Ortiz, Q. Cui, A.G. Baboul, S. Clifford, J. Cioslowski, B.B. Stefanov, G. Liu, A. Liashenko, P. Piskorz, I. Komaromi, R.L. Martin, D.J. Fox, T. Keith, M.A. Al-Laham, C.Y. Peng, A. Nanayakkara, M. Challacombe, P.M.W. Gill, B. Johnson, W. Chen, M.W. Wong, C. Gonzalez, J.A. Pople, Gaussian 03, Revision D.01, Gaussian, Inc., Wallingford CT, 2005.
[46] G. Schaftenaar, Molden V4.2, Program CAOS/CAMM Center Nijmegen Toernooiveld, 1991 Nijmegen, The Netherlands.
[47] E.C. Niederhoffer, A.E. Martell, P. Rudolf, A. Clearfield, Tris(1,10-phenanthroline) cobalt(III) triperchlorate dihydrate, $[Co(C_{12}H_8N_2)_3].2H_2O$, Cryst. Struct. Communic. 11 (1982) 1951–1957.
[48] Q.L. Zhang, J.H. Liu, X.Z. Ren, C.H. Li, P.X. Zhang, J.Z. Liu, L.N. Ji, A newly designed off-on luminescent probe formed by polypyridyl cobalt(III) complex and Zn^{2+}, Chinese. J. Inorg. Chem. 22 (2006) 885–889.
[49] X.H. Zou, B.H. Ye, H. Li, Q.L. Zhang, H. Cao, J.G. Liu, L.N. Ji, X.Y. Li, The design of new molecular "light switches" for DNA, J. Biol. Inorg. Chem. 6 (2001) 143–150.
[50] N. Kurita, K. Kobayashi, Density functional MO calculation for stacked DNA base-pairs with backbones, Comput. Chem. 24 (2000) 351–357.
[51] D. Řeha, M. Kabeláč, F. Ryjáček, J. Šponer, J.E. Šponer, M. Elstner, S. Sándor, P. Hobza, Intercalators. 1. Nature of stacking interactions between intercalators (ethidium, daunomycin, ellipticine, and 4',6-diaminide-2-phenylindole) and DNA base pairs. *Ab initio* quantum chemical, density functional theory, and empirical potential study, J. Am. Chem. Soc. 124 (2002) 3366–3376.
[52] H. Xu, K.C. Zheng, H. Deng, L.J. Lin, Q.L. Zhang, L.N. Ji, Effects of the ancillary ligands of polypyridyl ruthenium(II) complexes on the DNA-binding behaviors, New J. Chem. 27 (2003) 1255–1263.
[53] X.W. Liu, J. Li, H. Li, K.C. Zheng, H. Chao, L.N. Ji, Synthesis, characterization, DNA-binding and photocleavage of complexes $[Ru(phen)_2(6\text{–}OH\text{-}dppz)]^{2+}$ and $[Ru(phen)_2(6\text{–}NO_2\text{-}dppz)]^{2+}$, J. Inorg. Biochem. 99 (2005) 2372–2380.
[54] S. Shi, J. Liu, J. Li, K.C. Zheng, X.M. Huang, C.P. Tan, L.M. Chen, L.N. Ji, Synthesis, characterization and DNA-binding of novel chiral complexes Δ- and Λ-$[Ru(bpy)_2L]^{2+}$ (L=*o*-mopip and *p*-mopip), J. Inorg. Biochem. 100 (2006) 385–395.